Nonlinear Coda Wave Interferometry for the global evaluation of damage levels in complex solids

Yuxiang Zhang, Vincent Tournat, Odile Abraham, Olivier Durand, Stéphane Letourneur, Alain Le Duff, Bertrand Lascoup

Nonlinear coda wave interferometry for the global evaluation of damage levels in complex solids

Yuxiang Zhang[a,b], Vincent Tournat[a,*], Odile Abraham[b], Olivier Durand[b], Stéphane Letourneur[a], Alain Le Duff[a,c], Bertrand Lascoup[d]

[a]*LUNAM Université, LAUM, CNRS UMR 6613, Université du Maine, Av. O. Messiaen, 72085, Le Mans Cedex 9, France*
[b]*LUNAM Université, IFSTTAR, MACS, CS4, 44344, Bouguenais Cedex, France*
[c]*Groupe ESEO, 10 Boulevard Jeanneteau, CS 90717, 49107, Angers Cedex, France*
[d]*IRT Jules Verne, Chemin du Chaffault, 44340, Bouguenais, France*

Abstract

A nonlinear acoustic method to assess the damage level of a complex medium is discussed herein. Thanks to the highly nonlinear elastic signatures of cracks or, more generally, internal solid contacts, this method is able to distinguish between contributions from linear wave scattering by a heterogeneity and contributions from nonlinear scattering by a crack or unbounded interface. The coda wave interferometry (CWI) technique is applied to reverberated and scattered waves in glass plate samples featuring various levels of damage. The ultrasonic coda signals are recorded in both the absence and presence of an independent and lower-frequency elastic "pump" wave, before being analyzed by CWI. The monitored CWI parameters quantifying changes in these coda signals, which therefore quantify the nonlinear wave-mixing effects between the coda and pump waves, are found to be dependent on the damage level in the sample. A parametric study is also performed to analyze the influence of sensor positions and average temperature on the method's output. The reported results could be applied to the non-destructive testing and evaluation of complex-shape materials and multiple scattering samples, for which conventional ultrasonic methods show strong limitations.

1. INTRODUCTION

Due to their capacity for in-depth penetration and sensitivity relative to elastic properties, ultrasonic (US) wave methods are implemented in many fields (e.g. medicine, aeronautics, civil engineering) for non-destructive testing and evaluation (NDTE) applications. Standard US NDTE methods (including wave velocity monitoring and ultrasonic echo analysis) are proven to be effective and sufficient in many cases [1], especially when the tested medium is homogeneous. However, when the propagation media are complex, e.g. a multiple scattering medium, the application of standard US methods fails, mainly due to the quasi-exclusive use of coherent waves and their associated tools.

In the propagation of elastic waves, scattering event constitutes a primary cause of coherent acoustic energy attenuation (or geometric attenuation), which in turn leads to a loss of information when using conventional US methods. The occurrence rate of scattering events is typically characterized by t^*, the scattering mean free time (i.e. the average time between two scattering events) [2]. If the propagation time is longer than t^*, the coherent waves are strongly attenuated by scattering. To avoid such attenuation, conventional US methods almost exclusively employ waves with a propagation time of less than a few t^* (coherent waves). Due to the increased complexity of propagation media, which might result from a complicated geometry [3] or material heterogeneity [4, 5] (Figs. 1b and c), t^* can be considerably reduced, which would shorten the average life time of coherent waves as well. Consequently, the possibility for coherent waves to detect and characterize a defect at an unknown location or to thoroughly probe the entire medium when complexity is involved is smaller. One common solution employed in conventional US methods consists of expanding the wavelength in order to avoid scattering (thus increasing t^*) [6]. This approach however provides more a tradeoff than an actual solution, since the higher t^* comes at the expense of losing sensitivity and resolution capabilities. Conventional US NDTE methods are able to detect a defect through the accompanying ultrasound interaction, for which the wavelength should be comparable to the defect dimension, whereby "undersized defects" are barely even detected. The increased wavelength lowers sensitivity as more details become "undersized". Since defect detection relies on both the presence of ultrasound at the defect location (Fig. 1a) and the ultrasound-defect interaction efficiency, the performance of conventional US methods can thus be strongly limited within a complex medium.

The signal of multiply scattered waves (also referred to as incoherent waves or coda waves) is often overlooked by conventional US methods due to its noise-like appearance. Previous studies have shown however that this signal contains detailed information about the propagation medium and is highly repeatable [7, 8]. For these reasons, multiply scattered elastic waves are used to assess complex propagation media [9–12]. Its applications were later introduced into the NDTE field [3, 13, 14].

*Corresponding author
Email address: vincent.tournat@univ-lemans.fr (Vincent Tournat)

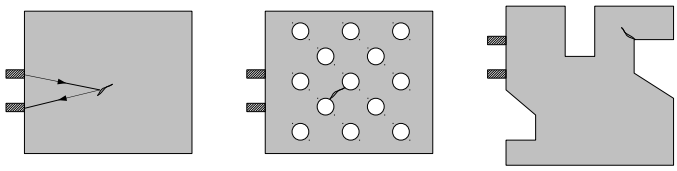

(a) (b) (c)

Figure 1: Illustration to determine the presence of cracks, i.e. localized nonlinear scatterers, in: (a) a homogeneous propagation medium with simple geometry; (b) an inhomogeneous propagation medium with a number of inclusions (linear scatterers) and a crack; and (c) a homogeneous propagation medium with complex geometry and a barely accessible crack.

The long-time propagation in multiple scattering media leads to propagation paths that are not only long but also well distributed spatially. It then becomes possible to probe the entire propagation medium in a global and repeated manner, even within areas that are beyond the reach of coherent waves (Fig. 1c). As the superposition of all scattered waves picked up by transducer, the recorded coda signal contains information collected from the entire medium, including the defect. The presence of a defect can ultimately be detected by analyzing coda signals according to various methods [15–19].

To expand the capacity of damage detection even further, our suggestion calls for combining the use of multiple scattered waves along with nonlinear acoustic effects: coda wave interferometry (CWI) technique [14] is thus associated with a nonlinear modulation effect [20–22]. In our previous study [23], it was demonstrated that global damage detection can be achieved by monitoring with CWI the nonlinear mixing effect caused by the presence of nonlinear scatterers (cracks) in an initially linear elastic medium (Pyrex glass). Under acoustic excitation, the presence of cracks is observed by their specific nonlinear behaviors [5, 24–30]. By sending high-amplitude waves over a broad frequency band, which includes multiple resonant frequencies of the sample, the nonlinear behavior of cracks can be triggered in most positions within the medium. Moreover, by thoroughly assessing the propagation medium using multiple scattered coda waves, the occurrence of such nonlinear modulation phenomena can then be detected in fine detail as pump amplitude-dependent variations of the CWI results.

In this study, our aim is to demonstrate a global evaluation of damage level by assessing the effective nonlinear level of the propagation medium using a nonlinear modulation of the coda waves and CWI analysis. We consequently denote the method implemented here as nonlinear coda wave interferometry (NCWI). In performing the set of previously described nonlinear tests on three Pyrex plates, identical at first but differently damaged with localized cracks, the effective nonlinear level, as quantified by NCWI-derived coefficients C_α and C_{Kd}, can be correlated with the level of damage, thus indicating the possibility of a damage level evaluation. A subsequent test demonstrates experimentally that such an effective nonlinear level is an intrinsic nonlinear parameter of the wave-material interaction, which solely depends on the level of damage and not on its location, hence confirming the global nature of the evaluation. As a practical matter, the experimental repeatability of this method and the influence of temperature changes have also been studied.

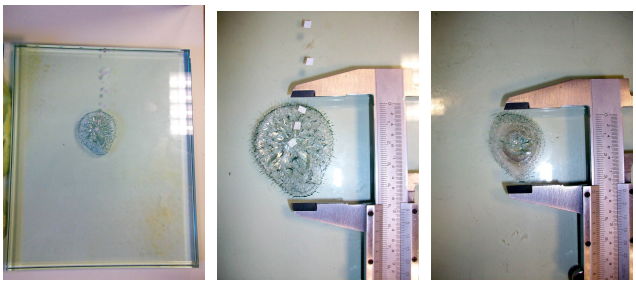

(a) (b) (c)

Figure 2: Pictures of the damaged samples: glass plates with dimensions of 1.6 cm × 23 cm × 19 cm, with two distinct levels of localized damage created artificially by thermal shock: (a) global view of the more heavily damaged sample; (b) close-up in the cracking zone of the more heavily damaged sample whose diameter equals approximately 5 cm; and (c) close-up in the cracking zone of the less damaged sample whose diameter is approximately 3.5 cm.

2. EXPERIMENTAL DESIGN

2.1. Specimen description

Three initially identical Pyrex glass plates (1.6 cm × 23 cm × 19 cm) were tested for purposes of this study. To differentiate test specimens by damage level, one specimen was left intact to serve as the reference, while the other two were artificially damaged by a localized thermal shock. Such a procedure causes a number of visible cracks within a finite volume of the specimen. A quasi-hemispherical cracked zone could be observed on the surface (Fig. 2a). According to the diameters of these cracked zones, the specimens can be considered to show different levels of damage: intact, less damaged, and more heavily damaged. The specimen displaying a cracked zone diameter of 5 cm was identified as the more heavily damaged and the specimen with a smaller zone (diameter: 3.5 cm) as the less damaged (Figs. 2b and c). The propagation of acoustic waves through the intact sample yielded velocities of ∼4,500 m/s for longitudinal waves and ∼2,750 m/s for shear waves. The quality factor of the intact sample at probe wave frequencies, evaluated via the exponential decrease of the late coda signals, is $Q \sim 200 \pm 30$.

2.2. Experimental set-up

Two types of piezoelectric transducers were used in these experiments. Transducers with a high working frequency range of 200-800 kHz (®Vermon type-M0.5/1070) were introduced for the excitation and detection of probe coda waves, hence their names probe emitters and probe receivers, respectively. The ®Ferroperm type-Pz26 transducers were used for generating larger-amplitude pump waves and are therefore called pump wave emitters. They operate over a lower frequency range, which is typically located between 15 kHz and 50 kHz. All transducers are glued onto the specimen edges with superglue.

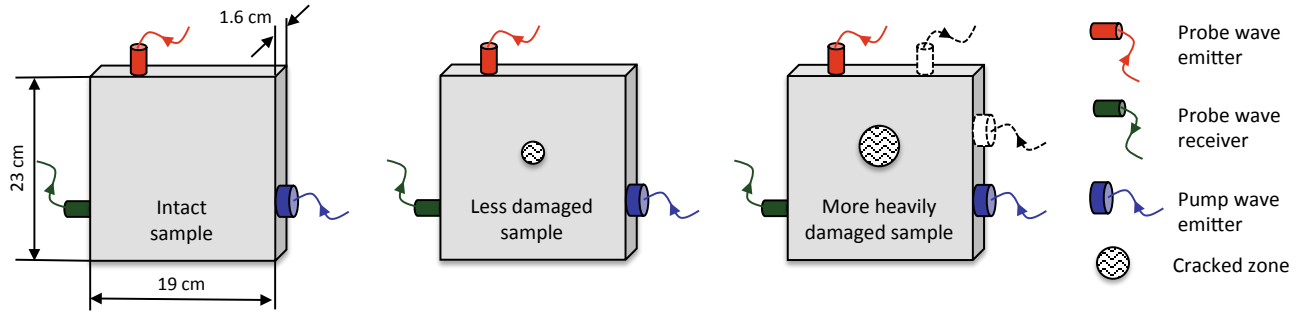

Figure 3: Schematic diagram of the experimental set-up - Glass plate samples (1.6 cm× 23 cm×19 cm) at three distinct levels of damage (intact, less damaged, more heavily damaged), with transducers serving different purposes being installed on their edges by gluing according to a similar configuration. Two transducers, illustrated by dashed lines, are glued onto the more heavily damaged sample but have not been used in this test; the purpose of their installation is detailed in Section 3.2.

The measurement system adopted for this study is the same as that described in [23]. Chirp signals with a frequency increasing from 200 to 800 kHz within 200 µs are generated, amplified and then sent into specimens via the probe wave emitter. Synchronized to each probe wave emission, the probe receiver picks up a 2-ms signal as a single acquisition at a 5-MHz sampling frequency and with 16-bit amplitude dynamics. To improve the signal-to-noise ratio, an average of 64 successive acquisitions is performed. With a repetition rate of 80 Hz, each coda signal is subsequently recorded within less than a second.

During the acquisition of probe waves, the acoustic pump waves are continuously launched into the specimens in the form of 11-ms linear chirp signals in the 15-50 kHz frequency range. It has been verified for each specimen that more than 10 resonant frequencies are present within this frequency range.The pump waves emission is not synchronized with that of probe waves for having the nonlinear effects well distributed on the successive coda acquisitions and eventually averaged on the retained coda signal [23].

The amplitude of the probing signal remains identical throughout the experiments, whereas the pump signal amplitude gets modified by manually altering the corresponding power amplifier gain (from 0 to 60 dB with an increment of 10 dB). Through measuring the out-of-plane velocity at different positions on the surface of the specimens using a laser vibrometer, the resulting strain amplitude corresponding to a 60 dB amplification gain is evaluated to be of the order of 10^{-6}, which is higher than that of the probe wave. The linear correlation between amplification gain and output amplitude has been verified, with the maximum amplitude of the pump signal corresponding to a 60-dB amplification gain equaling approx. 200 V peak-to-peak.

Experimental procedure for the nonlinear mixing tests

The key element in this study, namely the nonlinear mixing test, will now be described. Each nonlinear mixing test is composed of 16 steps and divided into three phases, in accordance with the pump wave amplitude A_{pump} protocol, i.e.:

- Phase 1, steps 1 through 7: A_{pump} is manually increased from 0 to 60 dB step-by-step with a 10-dB increment between each step;
- Phase 2: A_{pump} is constantly held at 60 dB for another four steps until reaching step 11;
- Phase 3: A_{pump} is directly lowered from 60 dB to 0 dB at the beginning of step 12 and then remains at this level during the last five steps

Each step lasts about 20 s, during which both pump waves and probe waves are repeatedly emitted into the specimens in an asynchronous manner while 10 coda signals are being recorded. Due to the absence of pump-probe synchronization and the fact that each coda signal is the average of 64 consecutive acquisitions, a uniformly-distributed and averaged nonlinear effect on the coda signals is ensured.

2.3. Signal processing and NCWI parameters

The signal processing method applied to coda signals stems from the CWI and is known as the *Stretching* method [31]. Each group of 160 coda signals recorded during a given test is analyzed in order to evaluate variations in propagation velocity and waveform. The first signal of each group, which is recorded with A_{pump}=0 dB, is set as the reference signal $h_0[t]$, and propagation velocity v_0 is considered as the reference velocity. By dilating/compressing $h_0[t]$ with a dilatation parameter τ_i, it is possible to simulate a signal ($h_0[t(1+\tau_i)]$) that would correspond to the propagation taking place in the same medium yet with a modified wave velocity $v_0(1+\tau_i)$. This simulated signal is then compared to $h_1[t]$, which has been recorded experimentally in the propagation medium assumed to be perturbed (in this study, it is being perturbed by the pump wave). Such a comparison is drawn by evaluating the correlation coefficient CC between signals $h_0[t(1+\tau_i)]$ and $h_1[t]$ within the time window [$t1$, $t2$]:

$$CC^{(t_1,t_2)}_{(h_0,h_1)}(\tau_i) = \frac{\int_{t_1}^{t_2} h_0[t(1+\tau_i)] \cdot h_1[t]dt}{\sqrt{\int_{t_1}^{t_2} h_0^2[t(1+\tau_i)]dt \cdot \int_{t_1}^{t_2} h_1^2[t]dt}}. \quad (1)$$

The time window in this study is selected as [1, 1.25] ms. Given the experimental setup, this selection ensures that the propagation time is long enough for ultrasonic waves to probe the entire medium thoroughly, and that the window is wide enough for CWI to be efficiently applied.

The value of τ_i that maximizes $CC^{(t_1,t_2)}_{(h_0,h_1)}(\tau_i)$ is denoted α; this value corresponds to a perturbed-state propagation velocity of $v_1 = v_0(1+\alpha)$ and is therefore considered to be the relative variation in effective propagation velocity $\alpha = \frac{v1-v0}{v_0}$. The second parameter deduced from the analysis is:

$$\mathrm{Kd} = 1 - CC^{(t_1,t_2)}_{(h_0,h_1)}(\alpha), \tag{2}$$

i.e. the remnant decorrelation coefficient that measures the level of waveform distortion between $h_0[t]$ and $h_1[t]$ within the selected time window.

3. EXPERIMENTAL RESULTS

3.1. Dependence on damage level

Three piezoelectric transducers (probe wave emitter, probe wave receiver and pump wave emitter) have been glued onto each of the three specimens according to a similar configuration (Fig. 3). The nonlinear mixing tests were performed by following the protocol described in Section 2.2. The pump wave amplitude (A_{pump}) for each step of the nonlinear mixing test is plotted in Fig. 4c. Experimental coda signals are then analyzed by running the *Stretching* method. In setting the first recorded signal as the reference, velocity variation α and remnant decorrelation coefficient Kd (as defined in the previous section) can be evaluated for every signal of the same test. The NCWI results of all three tests are illustrated in Figs. 4a and b, where α and Kd (obtained from 10 signals recorded during a single step) are represented by their average value as a color symbol (blue circle, green square or red pentagram).

NCWI results of the two damaged specimens clearly show the dependence of A_{pump}: in phase 1, as the level of A_{pump} increases, α decreases while Kd also increases; during phase 2, with A_{pump} held constant at 60 dB, both α and Kd stop changing and maintain their levels; and lastly in phase 3, as A_{pump} drops back to 0 dB, α and Kd return to their initial levels as well. Moreover, NCWI results of the intact sample indicate no comparable variations throughout the entire test. This result agrees with our previous study [23] and demonstrates that: 1) the glass can initially be considered as a linear elastic material for acoustic propagation; and 2) when specimens are damaged, cracks appear and play the role of nonlinear scatterers (sources) for the acoustic interaction between pump and probe waves.

By comparing the NCWI results of the two damaged specimens, it is clear that the probe wave in the more heavily damaged specimen is more sensitive to the presence of pump waves. Under the same level of A_{pump}, NCWI parameters of the more heavily damaged specimen reveal greater changes than those of the less damaged one. The α and Kd values obtained during phase 1 of each test are plotted in Fig. 5 vs. pump wave amplitude in order to illustrate the A_{pump} dependencies of NCWI parameters. For the sake of clarity, NCWI parameters have been plotted in a linear-linear scale by normalizing the pump wave amplitude to its lowest value A^*_{pump}=A_{pump}/A^{min}_{pump}.

The nonlinear mixing effects in both damaged specimens are exposed through the pump amplitude dependence of NCWI parameters. A linear relation of α *vs.* A^*_{pump} and a quadratic relation of Kd *vs.* A^*_{pump} are observed and can be expressed as

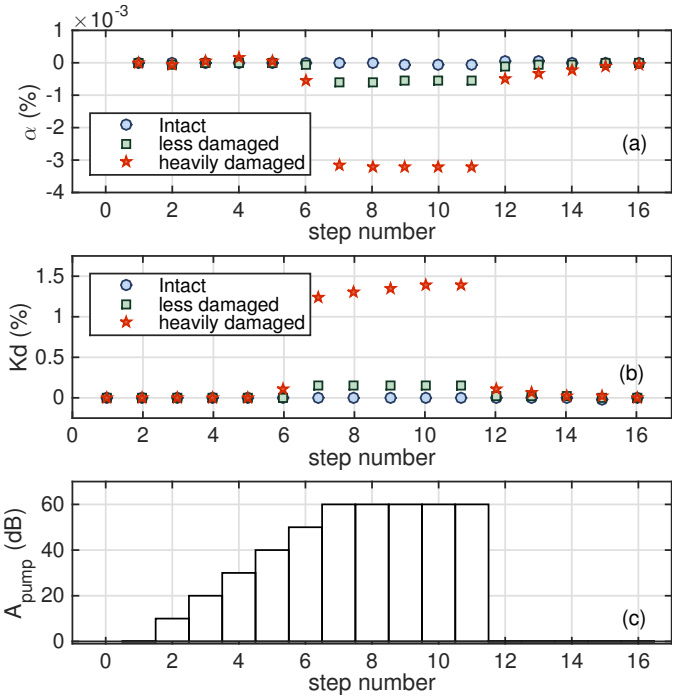

Figure 4: Damage dependence of the nonlinear acoustic mixing effect, as evaluated by CWI analysis: (a) Velocity variation α vs. step number; (b) Remnant correlation coefficient Kd vs. step number; and (c) Excitation amplitude of pump waves at each step of the test. The CWI results obtained on different specimens have been illustrated with the following color symbols: blue circles for the intact specimen, green squares for the less damaged specimen, and red pentagrams for the more heavily damaged specimen.

Nonlinear Coefficient	Intact	Less damaged	Heavily damaged
C_α	4.6 E-10	5.4 E-9	2.9 E-8
C_{Kd}	3.9 E-10	2.1 E-9	1.2 E-8

Table 1: Extracted nonlinear parameters C_α and C_{Kd} from the nonlinear wave mixing tests conducted on the three specimens with differing damage levels

follows:

$$\begin{aligned} \alpha &= -C_\alpha \cdot A^*{}_{pump} + R^0, \\ \mathrm{Kd} &= C_{\mathrm{Kd}} \cdot A^{*2}_{pump} + R^1 \cdot A^*_{pump} + R^0. \end{aligned} \tag{3}$$

The linear and quadratic parameters C_α and C_{Kd} can be extracted from the best fits; their values are listed in Table 1. Let's note that the terms with R^0 and R^1 are much smaller than the other terms in Eq. (3). In using the extracted values of Table 1, the various damage levels can be identified.

The glass samples are initially considered to be linear. The presence of cracks induced by the damaging mechanism causes localized nonlinearity, as a result of which the nonlinear mixing effect occurs between the probe coda wave and the pump wave. The use of multiple scattered coda waves as probe waves ensures a thorough inspection of the entire specimen by means of reverberation. The excitation of over 15 resonant modes of the sample by the pump wave also guarantees that the sample is excited everywhere with large-amplitude pump strains,

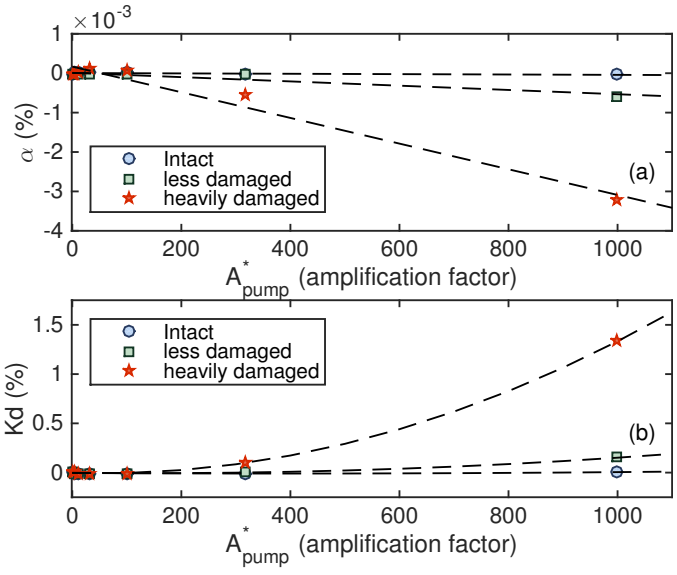

Figure 5: Pump amplitude dependence of NCWI parameters α and Kd for specimens with three distinct damage levels: (a) Velocity variation α vs. normalized pump amplitude; and (b) Remnant correlation coefficient Kd vs. normalized pump amplitude. The NCWI parameters obtained for the various specimens have been plotted with the following color symbols: blue circles for the intact specimen, green squares for the less damaged specimen, and red pentagrams for the more heavily damaged specimen; dashed lines display the linear and quadratic fits as a function of pump amplitude.

as described in [23]. The A_{pump}-dependent variations of NCWI parameters (α and Kd), as quantified by C_α and C_{Kd}, offer a global observation of the nonlinear mixing effects. The level of such effects depends simultaneously on the nonlinearity level of cracks (which, in our case, is assumed to be similar for both damaged samples since they were produced according to the same protocol), the extent and crack density of the damaged zone, and the level of pump acoustic excitation being applied. Given our ability to control the pump excitation amplitude, the values of C_α and C_{Kd} are thus closely correlated with the damage level of the sample.

3.2. *Validation of the global evaluation*

The conclusion of the previous section relies on the assumption that the effective nonlinear coefficients (C_α and C_{Kd}) deduced from NCWI results represent the effective nonlinear level of the specimen. As a global measurement of intrinsic properties, these coefficients characterize the nonlinear level of the structure as a whole. Their values therefore should not depend on the exact locations where coda measurements are taken or where the acoustic excitation is produced. To verify the global nature of the inspection method and confirm the conclusion drawn in Section 3.1, the following experiment has been conducted.

In this experiment, three probe transducers and two pump transducers were glued onto the more heavily damaged specimen (Fig. 6), even though nonlinear mixing tests require only three transducers (i.e. probe emitter, probe receiver and pump emitter). The two extra devices are installed to allow for a change in position of either the pump wave emitter or the

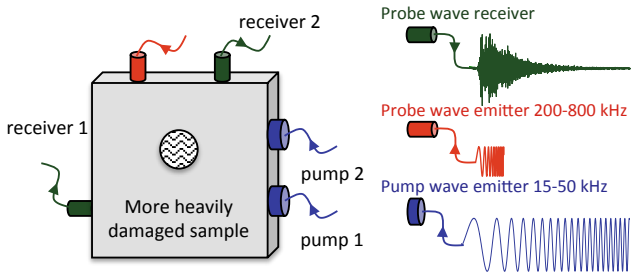

Figure 6: Schematic diagram of the experimental set-up - Three identical transducers of central frequency ~ 500 kHz are used for the probe coda wave measurement (chirp: 200-800 kHz) as one emitter plus two receivers, while two other identical transducers are used to generate the pump acoustic excitation at lower frequencies (frequency-swept signal between 15 kHz and 50 kHz).

probe wave receiver. Towards this end, three tests were performed using the measurement configurations listed in Table 2, which have been named accordingly R_{c1p1}, R_{c1p2} and R_{c2p2}. All five transducers were glued onto the specimen before the experiment, making it possible to consider such a specimen-transducers system as a signal structure that remains identical for all three tests.

Test	Probe wave receiver	Pump wave emitter
R_{c1p1}	n°1	n°1
R_{c1p2}	n°1	n°2
R_{c2p2}	n°2	n°2

Table 2: Measurement configurations of the three nonlinear mixing tests performed with various positions of the pump wave emitter or probe wave receiver

NCWI parameters for the increasing excitation phase (Phase 1) of each test have been plotted in Fig. 7. Results obtained from the intact and less damaged specimens in Section 3.1 are also shown for purposes of comparison. As previously anticipated, NCWI results display limited spatial dependence on transducer position, particularly that of the pump wave emitter. The changing position of the probe transducer between R_{c1p2} and R_{c2p2} exerts almost no influence since the corresponding results of the NCWI analysis are nearly identical (the red asterisks and red diamonds in Figs. 7a and b are difficult to distinguish). Meanwhile, the changing position of the pump transducer demonstrates greater importance since the NCWI results of test R_{c1p1} (red pentagrams) are visibly distinct from those of R_{c1p2} and R_{c2p2} (Fig. 7b). However, the NCWI parameter changes due to the fact that transducer positions on the samples are much smaller than the changes associated with damage levels for the tested samples (see Tables 1 and 3).

The results of this experiment indicate the robustness of the NCWI parameters obtained for a given sample and moreover demonstrate the global inspection aspect of the method.

3.3. *Influence of temperature on the method*

In the case of NDTE techniques, method robustness, i.e. experimental repeatability under varying external conditions, is

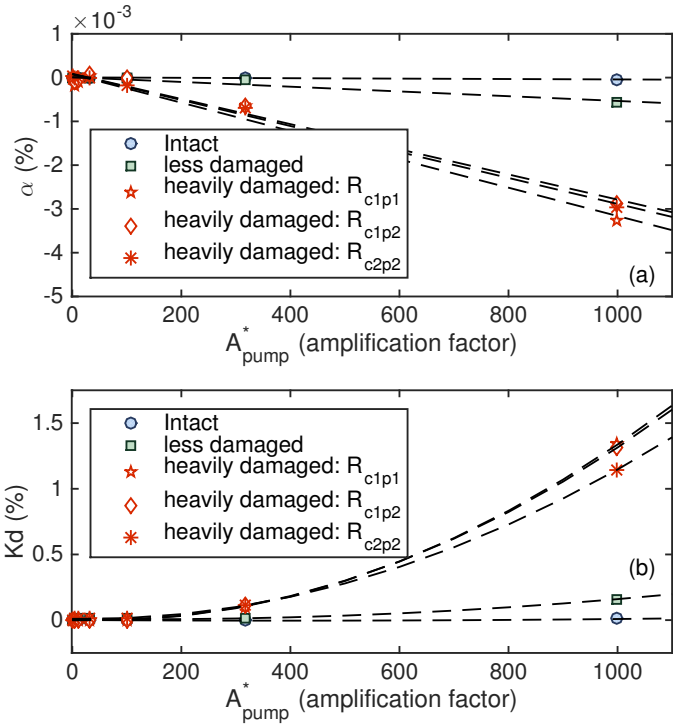

Figure 7: Comparison of nonlinear acoustic mixing effects resulting from changes in damage level and transducer position: (a) Velocity variation α vs. normalized pump amplitude; and (b) Remnant correlation coefficient Kd vs. normalized pump amplitude. The CWI parameters obtained for the various specimens have been illustrated with different colors, i.e.: blue circles for the intact specimen, green squares for the less damaged specimen, and red pentagrams, diamonds and asterisks for the three tests on the more heavily damaged specimen; dashed lines depict the linear and quadratic fits as a function of pump amplitude.

of interest along with method sensitivity. As one of the most frequently encountered environmental variables, ambient temperature changes might considerably influence the results of acoustic tests and, consequently, degrade method reliability. Let's note that linear ultrasonic CWI is so sensitive to effective wave velocity changes that in turn it becomes very sensitive to any temperature change [3, 32]. With the present method, the impact of temperature changes is considered from two different angles: 1) an experimental one, whereby its influence might affect the entire experimental set-up, which would cause thermal bias and ultimately degrade experimental repeatability [33]; and 2) a physical one, given the possibility that material nonlinearity might depend on temperature, which could cause difficulties in distinguishing the damage level from the

Nonlinear	Heavily damaged		
Coefficient	R_{c1p1}	R_{c1p2}	R_{c2p2}
C_α	2.9 E-8	2.9 E-8	2.7 E-8
C_{Kd}	1.4 E-8	1.2 E-8	1.2 E-8

Table 3: Experimental results of nonlinear parameters C_α and C_{Kd} of the more heavily damaged specimen in three nonlinear tests (the pertinent configurations are listed in Table 2)

effective nonlinearity level. To address this issue, experimental studies have been conducted to verify the influence of temperature on our method.

Three nonlinear mixing tests have been simultaneously performed on all three specimens: the more heavily damaged and intact specimens were installed in a climate chamber, while the less damaged specimen was simply placed outside the chamber without any temperature controls. For these three tests, temperature in the climate chamber was set at 20°C, 30°C and 40°C, respectively. A 3-hour relaxation period was inserted between successive tests so that temperature in the specimens could stabilize. With such temperature variations, the thermal dependence of the tested nonlinear elastic damage was expected to be revealed. Also, the results obtained from the less damaged specimen could be utilized to demonstrate experimental repeatability under laboratory conditions. The experimental results of all three tests are exhibited in Fig. 8 for the sake of comparison, and the corresponding extracted nonlinear coefficients are summarized in Table 4.

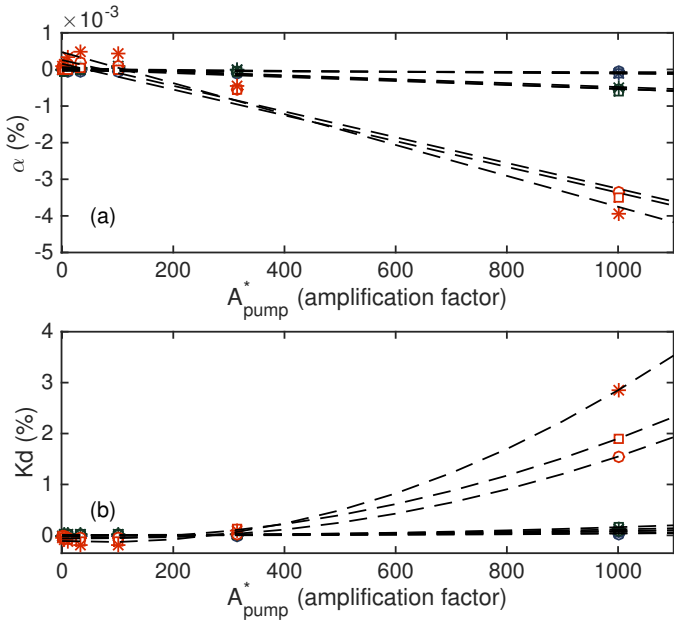

Figure 8: Comparison of nonlinear acoustic mixing effects resulting from changes in damage level and temperature: (a) Velocity variation α vs. normalized pump amplitude; and (b) Remnant correlation coefficient Kd vs. normalized pump amplitude. The three colors blue, green and red stand for NCWI result in the intact, less damaged and more heavily damaged specimens, respectively; the three symbols with the same color (circle, square and asterisk) indicate results obtained in tests 1, 2 and 3, respectively; dashed lines depict the linear and quadratic fits as a function of pump amplitude.

Satisfactory experimental repeatability has been confirmed by results on the less damaged specimen since both nonlinear coefficients show just a slight difference (Table 4); moreover, the corresponding curves in Fig. 8 practically overlap. Due to a forced temperature change in the climate chamber, NCWI results in the other two specimens display greater variations. From a visual comparison, α appears to be less influenced by temperature, with the three damage levels being easily identified in Fig. 8a. The Kd results from both the intact and less dam-

aged specimens however are difficult to distinguish in Fig. 8b using the adopted scale. Nevertheless, they are distinguishable by the change in order of magnitude in the extracted nonlinear coefficients, as provided in Table 4.

4. Conclusion and discussion

This work has reported on the application of a previously developed method for the global evaluation of damage levels in reverberating or multiple scattering media. Three initially identical Pyrex glass plates were tested, with two of them having been damaged by thermal shocks, thus leading to a number of visible cracks concentrated in a small portion of the samples. Sending high-amplitude, frequency-swept pump waves into the samples serves to modify the medium's elasticity at its highest susceptibility locations, namely where the cracks are located (and, by definition, where elastic nonlinearity is greatest). This nonlinear behavior can then be observed in fine detail by NCWI applied on the signals of higher-frequency, reverberated coda waves. The results presented as A_{pump}-dependent variations of α and Kd indicate linear and quadratic dependencies, respectively. From such dependencies, an effective nonlinearity level is evaluated by nonlinear coefficients C_α and C_{Kd}. As demonstrated experimentally, such an evaluation assesses the overall sample; the results obtained depend solely on the damage level and remain independent of damage location. We have therefore concluded that the extracted nonlinear parameters can be used to monitor/evaluate the damage level of a complex structure from a global perspective.

Because temperature variations are known to strongly alter the benefits and sensitivity of CWI methods, the influence of temperature has also been analyzed for the reported method and damaged samples. It has been demonstrated under laboratory conditions that this method offers satisfactory experimental repeatability, and the various damage levels are still clearly identified even when controlling for relatively sizable temperature modifications (10°C and 20°C). Let's observe that the effective nonlinear parameters C_α and C_{Kd} are orders of magnitude less sensitive to temperature change than α and Kd. Nonetheless, a limited influence of temperature change on the effective nonlinear coefficients does exist, and it appears that C_α is less sensitive to temperature change than C_{Kd}. Although no clear pattern between temperature change and the value of nonlinear coefficients has been detected in our study, a more detailed parametrical assessment of the nonlinearity of thermal dependence should be envisioned in the future.

We chose Pyrex glass for our specimens mainly because it can be damaged with real cracks and visually examined. The method developed can be applied to other materials, whether initially linear or not. In a recent study, this method had already been successfully applied on concrete samples to detect closed cracks [34], in which case undamaged concrete is already weakly nonlinear and cracks caused by mechanical damage further increase the sample's effective nonlinearity being probed by the method. Depending on its origin, damage can be global or local in concrete. Compared to NDT&E methods that are based on similar nonlinear elastic phenomena, e.g. Nonlinear Elastic Wave Spectroscopy [35] or Nonlinear Resonant Ultrasound Spectroscopy [36], the described method presents an improved capability on detecting globally in a sample (i.e. without low sensitivity zone) a localized damage. Moreover, it could be adapted with an imaging technique developed for diffuse waves [37] in order to map the effective nonlinearity within a multiple scattering medium (e.g. by imaging velocity change under pump acoustic excitation). With a local increase of effective nonlinearity caused by local damage, the latter in a multiple scattering medium could thus be detected and located simultaneously, without requiring any prior monitoring or threshold value.

5. Acknowledgments

This research was supported by the ECND-PdL (a cluster of laboratories dedicated to the issue of Non Destructive Evaluation and Control) and by LMAc project 2IDANL, funded by the Région Pays-de-la-Loire. Our thanks are extended to Robert Sachs, a native English speaker commissioned to proofread the final version of this paper.

References

[1] H. Wiggenhauser, Advanced NDT methods for the assessment of concrete structures, in: H. D. F. M. P. Alexander MG; Beushausen (Ed.), 2nd Int. Conf. Concr. Repair, Rehabil. Retrofit., 10 m, pp. 21–34.
[2] V. Rossetto, L. Margerin, T. Planes, E. Larose, Locating a weak change using diffuse waves: Theoretical approach and inversion procedure, J. Appl. Phys. 109 (2011) 034903.
[3] R. L. Weaver, O. I. Lobkis, Temperature dependence of diffuse field phase, Ultrasonics 38 (2000) 491–494.
[4] R. L. Weaver, W. Sachse, Diffusion of ultrasound in a glass bead slurry ultrasonic, J. Acoust. Soc. Am. 97 (1995) 2094–2102.
[5] V. Tournat, V. E. Gusev, Nonlinear effects for coda-type elastic waves in stressed granular media, Phys. Rev. E 80 (2009) 011306.
[6] T. Planès, E. Larose, A review of ultrasonic Coda Wave Interferometry in concrete, Cem. Concr. Res. 53 (2013) 248–255.
[7] M. Campillo, A. Paul, Long-range correlations in the diffuse seismic coda, Science 299 (2003) 547–549.
[8] A. Grêt, Time-Lapse Monitoring with Coda Wave Interferometry, Ph.D. thesis, Colorado School of Mines, 2004.
[9] E. P. Papadakis, Ultrasonic attenuation caused by scattering in polycrystalline metals, The Journal of the Acoustical Society of America 37 (1965) 711–717.
[10] K. Aki, B. Chouet, Origin of coda waves: Source, attenuation, and scattering effects, Journal of Geophysical Research 80 (1975) 3322–3342.
[11] R. L. Weaver, On diffuse waves in solid media, J. Acoust. Soc. Am. 71 (1982) 1608–1609.
[12] G. Poupinet, W. L. Ellsworth, J. Frechet, Monitoring velocity variations in the crust using earthquake doublets: An application to the Calaveras Fault, California, J. Geophys. Res. 89 (1984) 5719.
[13] K. Goebbels, Structure analysis by scattered ultrasonic radiation, Research Techniques in Nondestructive Testing 4 (1980) 87–157.
[14] R. Snieder, A. Grêt, H. Douma, J. Scales, Coda wave interferometry for estimating nonlinear behavior in seismic velocity, Science 295 (2002) 2253–2255.
[15] J. E. Michaels, T. E. Michaels, Detection of structural damage from the local temporal coherence of diffuse ultrasonic signals, IEEE Trans. Ultrason. Ferroelectr. Freq. Control 52 (2005) 1769–1782.
[16] E. Larose, T. Planes, V. Rossetto, L. Margerin, Locating a small change in a multiple scattering environment, Appl. Phys. Lett. 96 (2010) 204101.

	Temperature in thermostat	Intact specimen	Less damaged specimen	Heavily damaged specimen
Nonlinear coefficient: C_α				
Test 1	20°C	2.3 E-10	5.9 E-9	3.6 E-8
Test 2	30°C	6.4 E-10	5.5 E-9	3.4 E-8
Test 3	40°C	8.6 E-10	5.4 E-9	4.0 E-8
Nonlinear coefficient:C_{Kd}				
Test 1	20°C	4.9 E-10	1.1 E-9	2.2 E-8
Test 2	30°C	3.6 E-10	1.2 E-9	2.4 E-8
Test 3	40°C	6.0 E-10	2.1 E-9	4.2 E-8

Table 4: Nonlinear coefficients C_α and C_{Kd} quantifying the dependencies between NCWI results (α, Kd) and pump wave amplitude A_{pump}, for the three damaged specimens and three temperatures. Let's note that the less damaged specimen was not subjected to the indicated temperature changes since it was placed outside the climate chamber.

[17] C. Payan, V. Garnier, J. Moysan, P. A. Johnson, Determination of third order elastic constants in a complex solid applying coda wave interferometry, Appl. Phys. Lett. 94 (2009) 11904.

[18] C. Payan, V. Garnier, J. Moysan, Determination of nonlinear elastic constants and stress monitoring in concrete by coda waves analysis, Eur. J. Environ. Civ. Eng. 15 (2011) 519–531.

[19] A. Quiviger, C. Payan, J.-F. Chaix, V. Garnier, J. Salin, Effect of the presence and size of a real macro-crack on diffuse ultrasound in concrete, NDT&E Int. 45 (2012) 128–132.

[20] D. Donskoy, A. Sutin, A. Ekimov, Nonlinear acoustic interaction on contact interfaces and its use for nondestructive testing, NDT&E Int. 34 (2001) 231–238.

[21] K. E.-A. Van Den Abeele, P. A. Johnson, A. Sutin, Nonlinear Elastic Wave Spectroscopy (NEWS) Techniques to Discern Material Damage, Part I: Nonlinear Wave Modulation Spectroscopy (NWMS), Res. Nondestruct. Eval. 12 (2000) 17–30.

[22] V. Y. Zaitsev, L. A. Matveev, A. L. Matveyev, Elastic-wave modulation approach to crack detection: Comparison of conventional modulation and higher-order interactions, NDT&E Int. 44 (2011) 21–31.

[23] Y. Zhang, V. Tournat, O. Abraham, O. Durand, S. Letourneur, A. Le Duff, B. Lascoup, Nonlinear mixing of ultrasonic coda waves with lower frequency-swept pump waves for a global detection of defects in multiple scattering media, J. Appl. Phys. 113 (2013) 064905.

[24] Y. Zheng, R. G. Maev, I. Y. Solodov, Nonlinear acoustic applications for material characterization: A review, Can. J. Phys. 77 (2000) 927–967.

[25] V. V. Kazakov, A. Sutin, P. A. Johnson, Sensitive imaging of an elastic nonlinear wave-scattering source in a solid, Appl. Phys. Lett. 81 (2002) 646–648.

[26] K. Van Den Abeele, Multi-mode nonlinear resonance ultrasound spectroscopy for defect imaging: an analytical approach for the one-dimensional case., J. Acoust. Soc. Am. 122 (2007) 73–90.

[27] T. J. Ulrich, P. a. Johnson, R. a. Guyer, Interaction dynamics of elastic waves with a complex nonlinear scatterer through the use of a time reversal mirror, Phys. Rev. Lett. 98 (2007) 1–4.

[28] R. A. Guyer, P. A. Johnson, Nonlinear Mesoscopic Elasticity: The Complex Behaviour of Rocks, Soil, Concrete, Wiley-VCH, first edition, 2009.

[29] N. Chigarev, J. Zakrzewski, V. Tournat, V. Gusev, Nonlinear frequency-mixing photoacoustic imaging of a crack, J. Appl. Phys. 106 (2009) 036101.

[30] A. Novak, M. Bentahar, V. Tournat, R. El Guerjouma, L. Simon, Nonlinear acoustic characterization of micro-damaged materials through higher harmonic resonance analysis, NDT&E Int. 45 (2012) 1–8.

[31] C. Sens-Schönfelder, E. Larose, Temporal changes in the lunar soil from correlation of diffuse vibrations, Phys. Rev. E 78 (2008) 045601.

[32] A. Mazzeranghi, D. Vangi, Methodology for minimizing effects of temperature in monitoring with the acousto-ultrasonic technique, Exp. Mech. 39 (1999) 86–91.

[33] Y. Zhang, O. Abraham, V. Tournat, A. Le Duff, B. Lascoup, A. Loukili, F. Grondin, O. Durand, Validation of a thermal bias control technique for Coda Wave Interferometry (CWI), Ultrasonics 53 (2013) 658–664.

[34] B. Hilloulin, Y. Zhang, O. Abraham, A. Loukili, F. Grondin, O. Durand, V. Tournat, Small crack detection in cementitious materials using nonlinear coda wave modulation, NDT&E Int. 68 (2014) 98–104.

[35] K. E.-a. Van Den Abeele, A. Sutin, J. Carmeliet, P. a. Johnson, Micro-damage diagnostics using nonlinear elastic wave spectroscopy (NEWS), NDT E Int. 34 (2001) 239–248.

[36] C. Payan, V. Garnier, J. Moysan, P. Johnson, Applying nonlinear resonant ultrasound spectroscopy to improving thermal damage assessment in concrete, The Journal of the Acoustical Society of America 121 (2007) EL125–EL130.

[37] Y. Zhang, T. Planès, E. Larose, A. Obermann, C. Rospars, G. Moreau, Diffuse ultrasound monitoring of stress and damage development on a 15-ton concrete beam, The Journal of the Acoustical Society of America 139 (2016) 1691–1701.